Soil inorganic carbon stock under different soil types and land uses on the Loess Plateau region of China

Wen-Feng Tan [a,b,*], Rui Zhang [a], Hua Cao [a], Chuan-Qin Huang [a], Qin-Ke Yang [a], Ming-kuang Wang [c], Luuk K. Koopal [b,d]

[a] State Key Laboratory of Soil Erosion and Dryland Farming on the Loess Plateau, Institute of Soil and Water Conservation, CAS and MWR, Yangling 712100, Shaanxi, China
[b] Key Laboratory of Arable Land Conservation (Middle and Lower Reaches of Yangtze River), Ministry of Agriculture, College of Resources and Environment, Huazhong Agricultural University, Wuhan 430070, China
[c] Fujian Academy of Agricultural Sciences, Fuzhou 350003, Fujian, China
[d] Laboratory of Physical Chemistry and Colloid Science, Wageningen University, Dreijenplein 6, 6703 HB Wageningen, The Netherlands

ARTICLE INFO

ABSTRACT

The soil carbon reservoir is the largest carbon reservoir in terrestrial ecosystems and consists of soil organic and inorganic carbon stocks. Previous studies have mainly focused on the soil organic carbon (SOC) stock, and limited information is available about the soil inorganic carbon (SIC) stock. The Chinese Loess Plateau (CLP), which is located in the arid and semi-arid region of China, is an important inorganic carbon reservoir, with a thick soil layer that is rich in calcium carbonate. However, there are few reports on the SIC stock and its spatial distribution in this region. In the current study, the SIC densities and stocks for various soil types and land use patterns were evaluated based on 495 profiles with 2470 soil samples across the CLP, which were collected from the Chinese Second National Soil Survey. The results showed that in the top 1 m of soil across the CLP, the average SIC density is 17.04 kg/m^2, and the total SIC stock is approximately 10.20 Pg C (1 Pg = 10^{15} g). The SIC stock of the CLP accounts for approximately 18.4% of the total SIC stock throughout China. The average values of the SIC stock in the 0–20, 20–50 and 50–100 cm depths of the CLP are 2.39, 2.92 and 4.89 Pg, respectively. Under different land use patterns, the order of the average SIC density is farmland ≈ grassland > forest in all soil layers. For the various soil types, the SIC density in the 0–100 cm layer is the highest in alkaline soil and lowest in subalpine meadow soil, whereas the SIC stock is highest in loessial soil, eolian sandy soil and sierozem, and the lowest in subalpine meadow soil. These differences are largely a result of the area occupied by each soil type and the climate conditions. The results of this study provide basic information about carbon reservoir in China and contribute to our understanding of the SIC stock on the CLP as it relates to the carbon balance of terrestrial ecosystems.

© 2014 Elsevier B.V. All rights reserved.

1. Introduction

As an important part of the global carbon cycle, the terrestrial carbon ecosystem affects not only the global carbon balance but also the global temperature change (Eswaran et al., 1993). Soils have the potential to mitigate atmospheric CO_2 concentrations through C sequestration with a maximum global potential estimate ranging from 0.45 to 0.9 Pg C (1 Pg = 10^{15} g) per year (Lal, 2004). The soil carbon reservoir consists of soil organic carbon (SOC) and soil inorganic carbon (SIC). Most attention has been given to SOC, mainly because for most regions SOC contributes more to the carbon content than SIC and SOC affects the soil adsorption of CO_2 and the soil density distribution (Fang et al.,
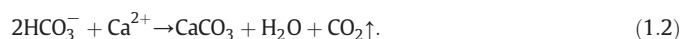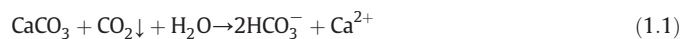
2001; Li et al., 2007, 2013; Liu et al., 2006, 2011; Wang and Zhou, 1999; Wang et al., 2012; Wu et al., 2003; Yu et al., 2007a, 2007b). However, in arid and semi-arid areas, which cover one third of the earth's surface, SIC is the dominant form of carbon (Lal and Kimble, 2000; Mi et al., 2008; Mielnick et al., 2005), and in these areas the SIC reservoir is approximately 2–10 times larger than that of SOC (Eswaran et al., 2000; Schlesinger, 1982).

The SIC reservoir consists mainly of carbonates (Schlesinger, 2002) and most research has been conducted on SIC in the form of carbonate (Li et al., 2007; Mi et al., 2008; Pan, 1999; Wu et al., 2009). SIC is divided into primary carbonate and secondary deposited carbonate (Ming, 2002). Primary carbonates are inherited from parent material of the soil. Secondary carbonates are formed through the dissolution and precipitation of carbonate parent material and derived from the weathering of calcium silicate. In the dissolution and precipitation of carbonate atmospheric CO_2 can be involved through a series of chemical reactions (Feng et al., 2001; Scharpenseel et al., 2000; Yang et al., 2010).
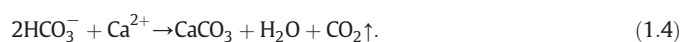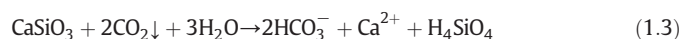
* Corresponding author at: Key Laboratory of Arable Land Conservation (Middle and Lower Reaches of Yangtze River), Ministry of Agriculture, College of Resources and Environment, Huazhong Agricultural University, Wuhan 430070, China.
E-mail address: wenfeng.tan@hotmail.com (W.-F. Tan).

In principal, one unit of CO_2 is consumed when one unit of carbonate is dissolved (Eq. (1.1)), and an equal amount of CO_2 is released when carbonate is re-deposited (Eq. (1.2)) (Wu et al., 2009):

$$CaCO_3 + CO_2\downarrow + H_2O \rightarrow 2HCO_3^- + Ca^{2+} \tag{1.1}$$

$$2HCO_3^- + Ca^{2+} \rightarrow CaCO_3 + H_2O + CO_2\uparrow. \tag{1.2}$$

Therefore, dissolution and precipitation of secondary carbonate balance each other with respect to atmospheric CO_2. The formation of secondary carbonate from calcium silicate also involves CO_2 (Emmerich, 2003; Goddard et al., 2007; Lal and Kimble, 2000; Wu et al., 2009). Atmospheric CO_2 can be fixed or released through, respectively, calcium silicate dissolution (Eq. (1.3)) and secondary carbonate deposition (Eq. (1.4)):

$$CaSiO_3 + 2CO_2\downarrow + 3H_2O \rightarrow 2HCO_3^- + Ca^{2+} + H_4SiO_4 \tag{1.3}$$

$$2HCO_3^- + Ca^{2+} \rightarrow CaCO_3 + H_2O + CO_2\uparrow. \tag{1.4}$$

Hence, weathering of a calcareous layer consumes 2 units of CO_2, but only 1 unit of CO_2 is released in the deposition of secondary carbonate. This can lead to the sequestration of atmospheric CO_2 in soils (Adams, 1993; Lal and Kimble, 2000; Wu et al., 2009). Next to the role of carbonate in fixation and release, it is also well known that the free form of carbonate affects soil oligomers, soil microbial activity, soil pH and the decomposition rate of soil organic matter. Furthermore, the SIC reservoir can be influenced by potential soil acidification through climate changes, for instance, the continuous acid deposition and agricultural activities. Such soil acidification can lead to large C losses from soil carbonates (Bowman et al., 2008; Entry et al., 2004; Mikhailova and Post, 2006; Papiernik et al., 2007; Sartori et al., 2007; Weng, 1995). Following Emmerich (2003), Singh et al. (2007) and Wu et al. (2001), it can thus be concluded that the SIC reservoir and its distribution play an important role in the dynamic changes of the atmosphere, the vegetation and the soil. Therefore, an accurate estimate of the SIC contribution to the soil carbon reservoir is required for a correct appreciation of the role of soils in the global ecosystem.

The Chinese Loess Plateau (CLP), located in the arid and semi-arid climate, covers a large area and, as such, is consequential to the global carbon cycles (Wang et al., 2011; Wen, 1989). Although investigations in China have been conducted on SIC on a national scale (Mi et al., 2008; Pan, 1999; Wu et al., 2009) and regional scale (Feng et al., 2001; Wang et al., 2013; Xu et al., 2009; Yang et al., 2010), the distribution of SIC on the integral CLP is largely unknown. Therefore, the aim of the present paper is to obtain more insight in the SIC reservoir of the CLP, which in turn will lead to a better understanding of the importance of the CLP for the global carbon cycles. The objectives of this study were (I) to estimate the SIC stock and SIC density in the 1 m soil horizon based on mainly 495 profiles with 2470 soil samples across the CLP collected from the Chinese Second National Soil Survey, and (II) to discuss the major factors that influence the SIC density and stock under different land uses, soil types and soil layers.

2. Materials and methods

2.1. Study area and data sources

The Chinese Loess Plateau (CLP) is located in the northwest of China (Fig. 1), which includes the upper and middle courses of the Yellow River (Shi and Shao, 2000). The plateau is surrounded by the Taihang mountain range to the east, Riyue–Helan Mountain to the west, the Qinglin range to the south and the Yinshan Mountain to the north (N33°43′–41°16′, E100°54′–114°33′). The CLP covers a total area of 620,000 km^2, with elevations ranging from 200 to 3000 m. The region is dominated by a temperate of arid and semi-arid continental monsoon climate. The mean annual temperature ranges from 3.6 to 14.3 °C, while the mean annual precipitation ranges from 150 to 800 mm. The precipitation occurs mainly between June and September, and decreases along a southeast to northwest transect (Yang and Shao, 2000). The vegetation zones occur in the following sequence: forest → forest-steppe →typical-steppe → desert-steppe → steppe-desert (Wang et al., 2010).

In this study, the soil data came mainly from the Second National Soil Survey in China, including Soil Species of China (NSSO, 1995a, 1995b, 1998) and the provincial soil survey (HNSSO, 2004; IMARSSO, 1994; Liu and Zhang, 1992; QARRPO, 1995). From the Second National Soil Survey 495 soil profiles (see Fig. 1 for the locations) were used. In total 2470 soil samples were collected over the soil horizons to analyze. Information in the database on the soil profiles include mostly profile depth, horizon thickness, organic matter content, calcium carbonate content, gravel content (particle diameter larger than 2 mm) and soil bulk density of the different horizons. These properties were determined by conventional methods (NSSO, 1998; Wu et al., 2009). Soil calcium carbonate was determined using the Chittick apparatus (Dreimanis, 1962). Soil organic carbon contents were determined by the potassium dichromate wet oxidation method (Walkley and Black, 1934). Soil bulk density was determined by the cutting ring method (Black and Hartge, 1986) and gravel content was measured using a 2-mm sieve. The data of the other surveys contained similar information.

The areas of each soil type were identified using the 1:500,000 Soil Map of the Chinese Loess Plateau, which is supplied by the Institute of Soil and Water Conservation, Chinese Academy of Sciences (CAS).

2.2. Data analysis

2.2.1. Calculation of the soil inorganic carbon content

To allow comparison with other studies, the calculation of the SIC stock in the present study is based on the soil profile data in the horizon of 0–100 cm. To obtain detailed information the soil profiles were subdivided into three standard horizons of 0–20 cm, 20–50 cm and 50–100 cm. In the soil survey data, the stratification of the soil profiles was often based on the characteristic soil horizons, and these did not necessarily coincide with the depth-based layers in the present study. Therefore, data of the pedogenetic horizons (i.e., O, A, B, C) were converted to depth-based layers. The calculation was based on the actual data for the different soil horizons. When the actual soil depth was deeper than 100 cm, only the $CaCO_3$ contents in the 0–100 cm horizons were used. When the actual depth of soil profiles in the soil survey data was less than 100 cm, the $CaCO_3$ content of the layer beneath the actual depth of the soil profile up to 100 cm was regarded as zero. During converting from pedogenetic horizons to three depth layers (0–20, 20–50, 50–100 cm), the depth of each horizon was used as a weighting coefficient according to their relative contributions to the overall depth, so as to derive the average $CaCO_3$ content of the soil profile to a depth of 20, 50 and 100 cm. For each soil profile the weighted $CaCO_3$ content by depth zone were calculated as product of depth of horizon, concentration of $CaCO_3$ and bulk density (Mi et al., 2008; Palmer et al., 2002). For example, to estimate inorganic carbon content in the 0–20 cm layer soil, the depth of the O horizon was used as the criterion to assign characteristics. When the thickness of O horizon was >20 cm, a layer of 20 cm was assumed with its characteristics equal to that of the O horizon. When the thickness of O horizon was <20 cm, an additional part from A horizon was taken with its properties to make up the 20 cm and average properties of the 0–20 cm layer were calculated from the weighted properties of the O horizon and the A horizon, weighting the amounts according to their relative contributions to the overall depth.

2.2.2. Calculation of soil bulk densities

In some cases soil density data were missing in the national soil survey but the soil organic carbon content (SOC) was known. In this case
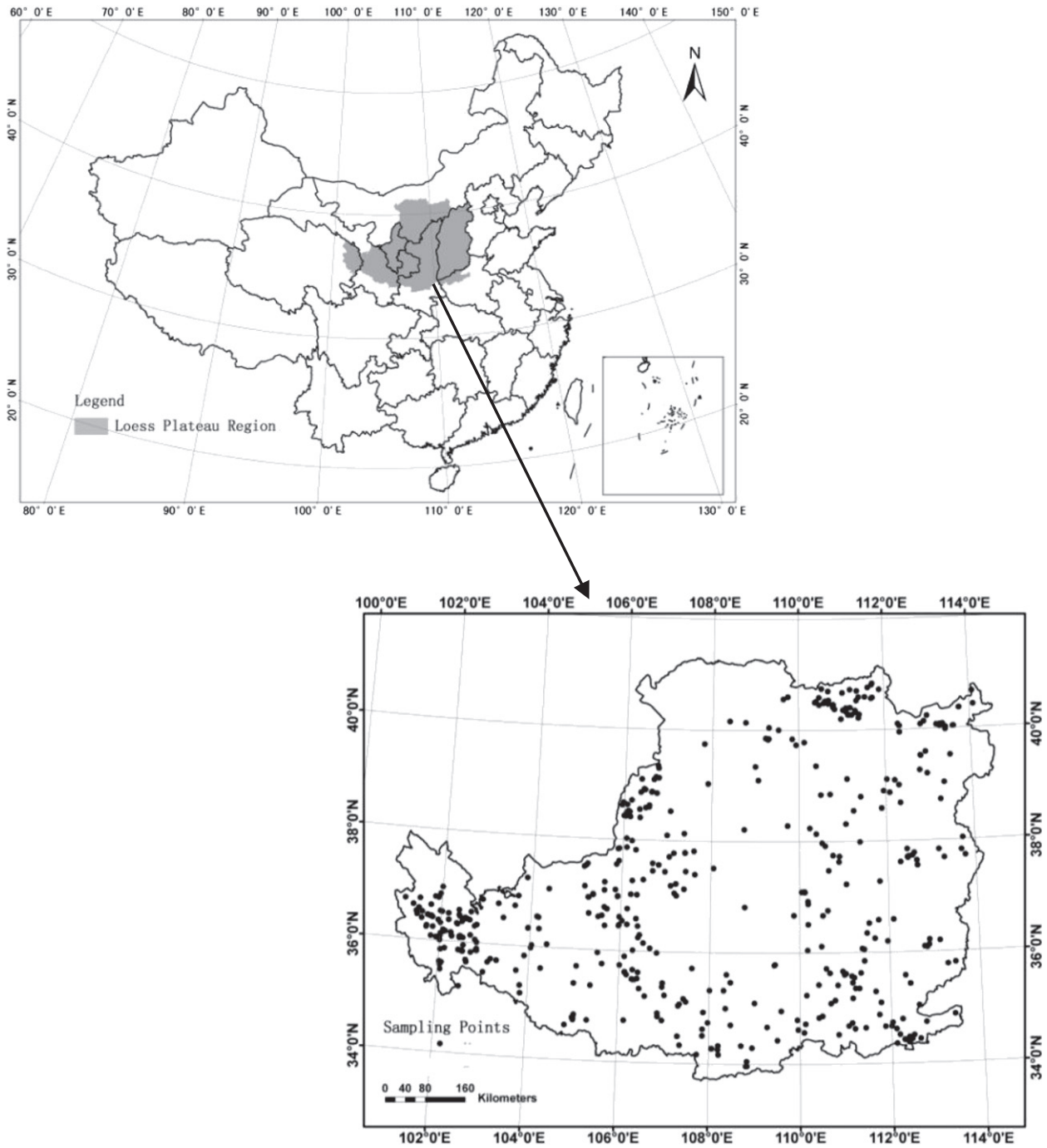
Fig. 1. The location of the Central Loess Plateau (CLP) in China; the distribution of the soil profiles is indicated in the enlarged image of the CLP.

the soil density was estimated from the SOC using an empirical function. The functional relationship between the *SOC* and soil bulk density (*D*) was established using the data from 167 soil samples. The data plot and regression curve are shown in Fig. 2, and the observed equation is:

$$D = -0.107 \ln(SOC) + 1.369 \tag{2.1}$$

where *D* is the soil bulk density in g/cm³, and '*SOC*' in %. For the soil profiles in which the soil bulk density was lacking, *D* was calculated by inserting the known *SOC* into Eq. (2.1).

2.2.3. Calculation of soil inorganic carbon densities

The soil inorganic carbon density (SICD) is the main parameter for the quantification of the total inorganic carbon storage (SICS). The inorganic carbon density of a soil layer *i* ($SICD_i$) is directly related to the soil properties according to Eq. (2.2):

$$SICD_i = 0.12(1-\theta_i) \times D_i \times C_i \times T_i/100 \tag{2.2}$$

where θ_i is the volume percentage of soil gravel fraction (particles > 2 mm), D_i is the average soil bulk density (g/cm³), C_i is the CaCO₃ content (g/kg) and T_i is the thickness (cm), all of layer *i*. The factor 0.12 is the ratio between the atomic mass of C and the molar mass of CaCO₃ and converts soil CaCO₃ to the soil inorganic C (Wu et al., 2009; Yang
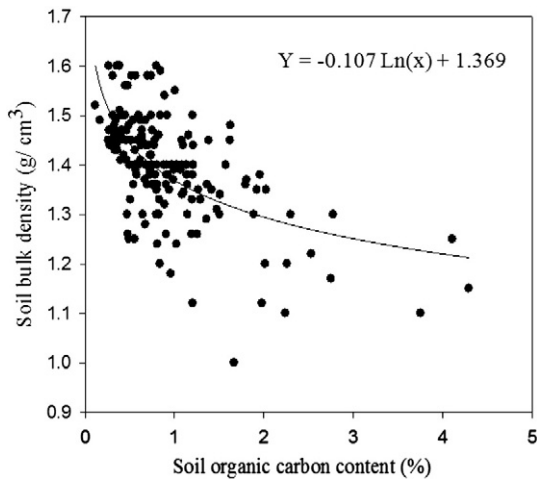
Fig. 2. Soil bulk density as a function of the soil organic carbon content on the CLP. The curve is the empirical relationship between the two properties (r = 0.3611, P < 0.01, and F = 93.24).

et al., 2012). When SI units are used, as indicated above, $SICD_i$ is obtained in kg C/m^2.

The total soil inorganic carbon density of a given soil profile is calculated using the summation of $SICD_i$ over all three layers in the 0–100 cm horizon:

$$SICD = \sum_{i=1}^{n} 0.12(1-\theta_i) \times D_i \times C_i \times T_i/100 \tag{2.3}$$

where $SICD$ is the total soil inorganic carbon density in a layer of 1 m and $n = 3$ is the number of layers.

The SICD of each soil type j was calculated as follows. (1) The SICD layer values per profile are calculated using Eqs. (2.2) and (2.3). (2) The profile sites that are covered by soil type j are established. (3) The average $SICD_j$ values of the three horizons and total layer are calculated using the data obtained in (1) and (2). When the data of a specific soil type were missing or insufficient, the $SICD_j$ values per layer of the unobserved soil or site were estimated as corresponding $SICD_j$ values nearby locations.

The soil types are discriminated on the basis of the genetic soil classification of China, this classification is correlated to the Chinese Soil Taxonomy (CRGCST, 2001). The latter can be compared to the WRB soil classification system and American Soil Taxonomy (CRGCST, 2001). The locations of the different soil types at the CLP can be obtained from the 1:500,000 Soil Map of the Chinese Loess Plateau. This map is based on the genetic soil classification of China.

In order to obtain a good impression of the spatial distribution of SICD on the CLP for the three different horizons and the total layer with 1 m, SICD maps of the CLP can be created for each layer. To generate these maps, the SICD data of the three horizons of the 495 profiles are used in combination with Kriging interpolation to establish the areal ranges over which the profile SICD values could be applied. The Kriging interpolation was used as a poplar geo-statistical approach to obtain upscale site-level data to regional-scale evaluation in soil carbon budgets (Yang et al., 2010, 2012). During spatial interpolation, a semi-variogram describing the relationship between the lag distance (x) and the semi-variance of underlying variable within the lag distance (y) was constructed to explore the spatial dependence in the underlying variable. The optimized semi-variogram, spatial interpolation and SICD maps was generated by using ArcGIS 9.3 (Cressie, 1993).

2.2.4. Calculation of soil inorganic carbon stock

The soil inorganic carbon stock of a given soil type j, $SICS_j$, is obtained by multiplying the $SICD_j$ of that soil with the area this soil covers. The

total $SICS$ for a region is obtained by summation of the inorganic carbon stock over all soil types j in that region:

$$SICS = \sum_{j=1}^{m} area_j \times SIDCD \tag{2.4}$$

where $SICS$ is the total inorganic carbon stock of a region, m is the number of soil types, and $area_j$ is the area of each soil type j with $SICD_j$. When SI units are used the $SICS$ is obtained in kg, however, commonly the SICS is expressed in Pg C (1 Pg = 10^{12} kg).

To obtain the soil areas per soil type the 1:500,000 Soil Map of the Chinese Loess Plateau was digitized and the different areas were obtained with an accuracy of about 1 km^2.

3. Results

3.1. Soil inorganic carbon density (SICD) of different soil types on the CLP

From the data for the 495 soil profiles with 2470 soil samples on the CLP the SICD distributions over the three sub-horizons were calculated for the different soil types as described above. The results are summarized in Table 1. Table 1 also includes the SICD values for the total 0–100 cm layer and the number of available profiles for each soil type is indicated. To give some insight in the range and frequency of SICD values observed for the profiles, the frequency distribution of SICD values was plotted in Fig. 3 for the three layers and for the total 0–100 cm horizon. Comparing the different layers it follows that the SICD in the CLP soil profiles increases with increasing depth. For the 0–20 cm, 20–50 cm and 50–100 cm layers the average SICD values were 3.31, 5.10 and 8.64 kg/m^2, respectively. The average SICD values of the 0–100 cm profiles ranged from 0 to 55 kg/m^2 with the most frequent values in the range of 6–23 kg/m^2 (Fig. 3). The average SICD in the 0–100 cm layer for all soil types was estimated to be 17.04 kg/m^2.

The range of the profile SICD values in the 0–100 cm layer is considerably larger than the range of average SICD values of the soil types (0.04 to 24.13 kg/m^2, see Table 1). The SICD of alkaline earth soil in the 0–100 cm horizon had the largest value (24.13 kg/m^2), while the subalpine meadow soil had the lowest value (0.04 kg/m^2). The SICD values of eight soil types (including irrigation-silted soil, loessial soil, sierozem, chestnut soil, bog soil, paddy soil, takyric solonetz, purple soil) were higher than the overall average SICD of 17.04 kg/m^2. Wu et al. (2009) have reported that the overall average SICD in the 0–100 cm soil layer for entire China is 6.3 kg/m^2. The average SICD value for the CLP is almost 2.7 times of the national SICD value, which is likely a result of the abundant eolian carbonate deposit on the CLP (Wu et al., 2009). Liu et al. (2011) have estimated that the soil organic carbon density on the CLP is 7.70 kg/m^2 in the 0–100 cm soil layer (Liu et al., 2011). Therefore, the contribution of inorganic carbon to total carbon on the CLP is about 69%.

The SICD distributions in the horizons of the various soil types on the CLP showed significant differences, which were mainly related to climate and parent material. The SICDs of the 0–20 cm horizon ranged from 0.00 to 24.07 kg/m^2, with an average of 3.31 kg/m^2. The most frequently observed range was 1–5 kg/m^2 (Fig. 3). The 0–20 cm average SICD of the northwestern CLP (>6.00 kg/m^2) was higher than that of the southeastern CLP. This difference in SICD values is mainly due to the increase in precipitation from northwest to southeast, which benefits the dissolution and leaching of CaCO$_3$. The average SICDs of the different soils ranged from 0 to 9.44 kg/m^2 in the 0–20 cm horizon (Table 1). The skeleton soil had the largest SICD value (9.44 kg/m^2), the alkaline earth soil had the second largest value (6.03 kg/m^2), and the lowest value occurred in the dark felty soil (about zero).

The SICDs of the 20–50 cm horizon ranged from 0.00 to 18.05 kg/m^2, with an average of 5.10 kg/m^2 and a clustering around 1–10 kg/m^2 (Fig. 3). In this horizon, the average SICD value of paddy soil was the

Table 1
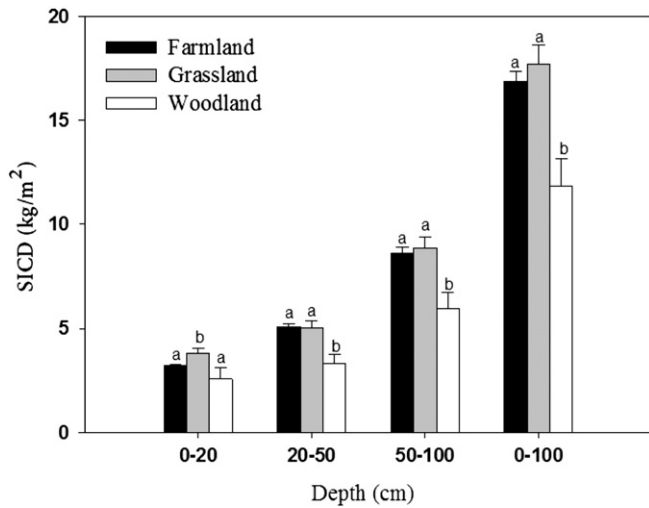Soil inorganic carbon density of different horizons and various soil types on the Chinese Loess Plateau.

Soil type		Number of profile	Soil inorganic carbon density (SICD, kg/m^2)			
Genetic soil classification of China	Chinese soil taxonomy		0–20 cm	20–50 cm	50–100 cm	0–100 cm
Aeolian sandy soil	Sandic Entisols	9	2.49 ± 0.55	2.85 ± 0.63	6.79 ± 1.30	12.13 ± 2.25
Alkaline earth soil	Alklic Halosols	3	6.03 ± 2.70	6.89 ± 2.11	11.21 ± 2.77	24.13 ± 7.54
Alluvic soil	Alluvic Entisols	20	3.17 ± 0.26	4.64 ± 0.49	5.77 ± 1.02	13.57 ± 1.58
Bog soil	Orthic Gleysols	8	5.78 ± 1.06	5.07 ± 0.99	8.16 ± 1.62	19.00 ± 3.25
Brown calcic soil	Hap-Orthic Aridisols	3	1.58 ± 0.60	3.96 ± 2.07	7.03 ± 2.27	12.57 ± 4.90
Brown soil	Hap-Udic Luvisols	8	0.02 ± 0.00	0.02 ± 0.01	0.02 ± 0.02	0.06 ± 0.04
Chernozem	Pac-Ustic Isohumosols	12	3.79 ± 0.90	3.35 ± 0.70	6.30 ± 1.20	13.45 ± 2.72
Chestnut soil	Cal-Ustic Isohumosols	59	3.38 ± 0.20	7.10 ± 0.37	12.71 ± 0.74	23.19 ± 1.08
Chestnut–cinnamon soil	Hap-Ustic Isohumosols	15	3.38 ± 0.28	5.11 ± 0.45	8.91 ± 0.82	16.59 ± 1.34
Chisley soil	Lit-Orthic Entisols	5	4.78 ± 0.28	/	/	4.78 ± 0.28
Cinnamon soil	Ustic Luvisols	60	2.50 ± 0.26	4.19 ± 0.41	8.26 ± 0.79	14.95 ± 1.16
Cold desert soil	Cryic Aridisols	1	0.18 ± 0.00	0.25 ± 0.00	/	0.44 ± 0.00
Dark felty soil	Mat-Cryic Cambisols	2	0.00 ± 0.00	0.55 ± 0.54	0.89 ± 0.89	1.45 ± 1.43
Dark loessial soil	Typ-Cum-Ustic Isohumosols	24	3.28 ± 0.35	4.27 ± 0.45	8.08 ± 0.85	15.63 ± 1.53
Gray desert soil	Hap-Orthic Aridisols	1	4.95 ± 0.00	5.16 ± 0.00	1.75 ± 0.00	11.86 ± 0.00
Irrigation-silted soil	Sil-Orthic Anthrosols	26	3.80 ± 0.16	6.33 ± 0.24	10.32 ± 0.63	20.44 ± 0.89
Loessial soil	Loe-Orthic Entisols	39	4.80 ± 0.30	6.48 ± 0.27	11.14 ± 0.38	22.42 ± 0.83
Lou soil	Earth-cumulic Orthic Anthrosols	13	3.33 ± 0.90	3.90 ± 0.64	5.49 ± 1.22	12.73 ± 2.07
Meadow soil	Udic Isohumosols	8	3.82 ± 0.93[‡]	4.11 ± 0.88	6.03 ± 1.25	13.96 ± 2.74
Moisture soil	Ustic Cambisols	80	2.98 ± 0.19	4.80 ± 0.30	8.14 ± 0.51	15.92 ± 0.90
Mountain meadow soil	Cry-Ustic Isohumosols	4	0.36 ± 0.34	0.55 ± 0.53	0.91 ± 0.88	1.82 ± 1.76
Paddy soil	Hap-Stagnic Anthrosols	7	3.96 ± 0.72	7.97 ± 1.41	11.90 ± 2.46	23.82 ± 4.34
Purple soil	Pur-Orthic Entisols	1	2.73 ± 0.00	5.52 ± 0.00	9.46 ± 0.00	17.71 ± 0.00
Red clay	Fer-Udic Luvisols	15	3.15 ± 0.67	3.86 ± 0.81	5.75 ± 1.43	12.76 ± 2.75
Saline soil	Orthic Halosols	3	3.21 ± 0.89	4.18 ± 0.46	7.09 ± 0.62	14.50 ± 1.96
Sierozem	Cal-Orthic Aridisols	62	3.52 ± 0.23	7.05 ± 0.32	11.34 ± 0.61	21.91 ± 0.90
Skeleton soil	Ari-Orthic Entisols	5	9.44 ± 4.02	2.73 ± 2.73	/[a]	12.16 ± 4.79
Subalpine meadow soil	Mol-Cryic Cambisols	2	0.02 ± 0.02	0.02 ± 0.02	0.00 ± 0.00	0.04 ± 0.04
Average across CLP		495	3.31 ± 0.58	5.10 ± 0.66	8.64 ± 0.97	17.04 ± 2.20

± means standard error.
[a] No data in this layer.
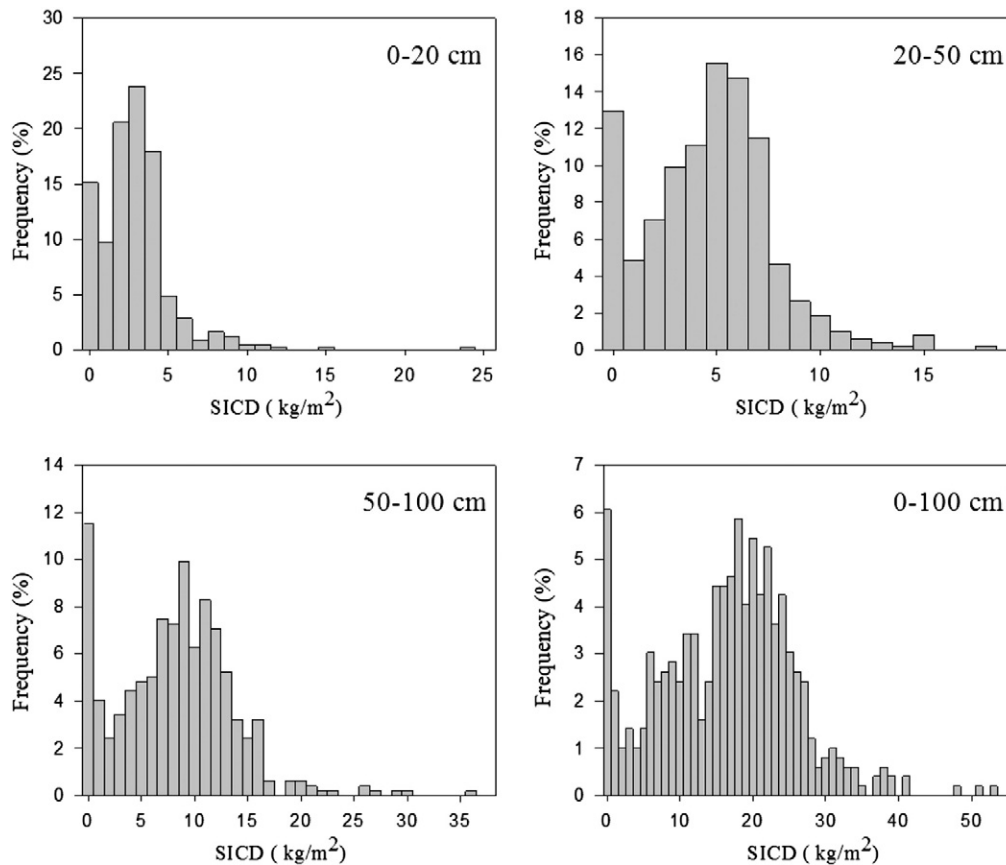
Fig. 3. Frequency distributions of SICD values observed for the various profiles at the CLP. The different distributions concern the different standard soil horizons (0–20 cm, 20–50 cm, 50–100 cm) and the total 0–100 cm horizon.

Fig. 4. Average soil inorganic carbon density in the 0–100 cm layer for different types of land use. Different letters denote significant differences in SICD under different land use types (LSD test; P < 0.05).

highest (7.97 kg/m^2), next was the chestnut soil (7.10 kg/m^2), and the brown soil (0.02 kg/m^2) was the lowest. The soils with relatively high SICD in the 20–50 cm horizon were primarily from Gansu, Qinghai, Ningxia, and upstate north Shaanxi. The high $CaCO_3$ contents of soils in these regions (e.g., irrigation-silted soil, loessial soil, sierozem, chestnut soil) could be attributed to the limited rainfall and relatively high rate of evaporation. Low SICD values were calculated for southern Shaanxi, Henan, and southern Shanxi, where rain fall caused frequent changes in soil moisture and relatively high carbonate leaching.

The SICDs of the 50–100 cm horizon ranged from 0.00 to 36.39 kg/m^2, with an average of 8.64 kg/m^2 and most frequent values of approximately 1 to 16 kg/m^2 (Fig. 3). The highest and lowest soil SICDs were for Chestnut soil (12.71 kg/m^2) and brown soil (0.02 kg/m^2), respectively.
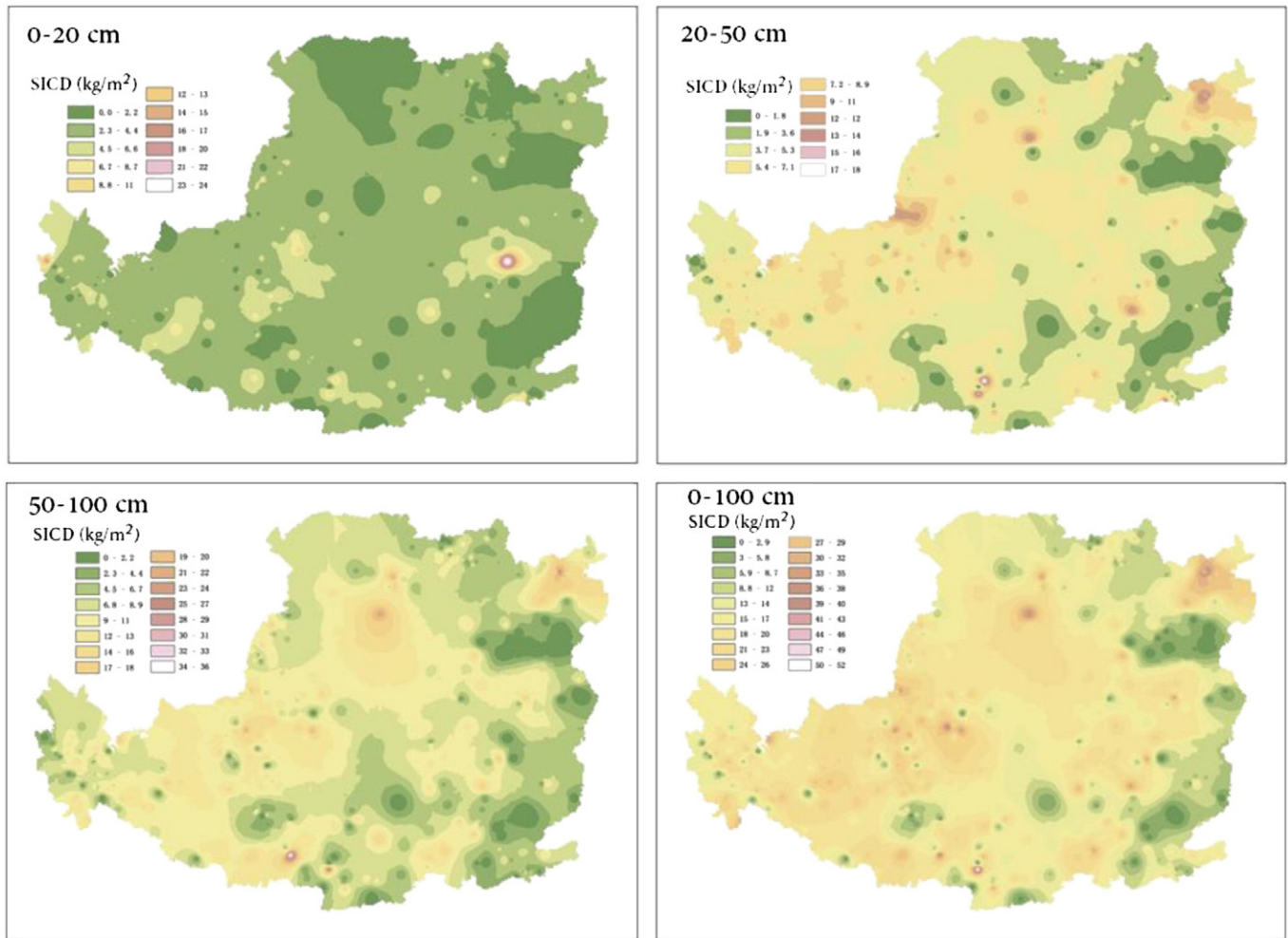
3.2. Soil inorganic carbon density (SICD) under different types of land use

According to the soil survey information, land use patterns are divided into farmland, grassland and woodland. In general, the distribution of SICD depends on land use, as different types of plant roots and organic carbon occur under different land use patterns (Jobbágy and Jackson, 2000). The SICD values for the different layers and different land use types are summarized in Fig. 4. The SICD follows the sequence: grassland ≈ farmland > woodland in all layers. Grassland is found mainly in the northwest and northern arid regions of the CLP, where relatively less carbonate leaching occurs due to the low precipitation and low temperature. Agronomic practices and conventional tillage of farmlands lead to processes that promote mineralization of soil organic matter and weathering of soil minerals. The soil organic carbon transforms from $C_{org.} \rightarrow CO_2 \rightarrow HCO_3^- \rightarrow CaCO_3$ (Pan et al., 2000; Xu and He, 1996), and weathering of soil minerals benefits the exchange of calcium in soils. These affect the reaction of carbonate with CO_2 (Velde and Meunier, 2008).

Woodland is mainly found in the southern region of the CLP, where intensive carbonate leaching occurs due to abundant rainfall and high temperatures. Although woodland is favorable for accumulation of organic matter, the many root exudates promote dissolution of carbonate and this leads to a lower SICD for woodland than for grassland or farmland.

3.3. Soil inorganic carbon stock (SICS) on the CLP

The areas covered by the different soil types on the CLP and the calculated SICS values for the different layers, as well as the entire 0–100 cm profile, are summarized in Table 2. For the whole profile (0–100 cm), the SICS in loessial soil was the highest (441.08 × 10^{10} kg), followed by eolian sandy soil (84.13 × 10^{10} kg) and sierozem (71.49 × 10^{10} kg). These high values are mainly a result of the large areas these soils occupy on the CLP. The SICS of sub-alpine meadow soil was the lowest (only 0.02 × 10^{10} kg), due to both the relatively low area occupied by this soil and the low SICD.

Table 2
Inorganic carbon stock of different horizons and various soil types on the Chinese Loess Plateau.

Soil type		Area	SIC stock (10^{10} kg)			
Genetic soil classification of China	Chinese soil taxonomy	(10^{10} m^2)	0–20 cm	20–50 cm	50–100 cm	0–100 cm
Eolian sandy soil	Sandic Entisols	6.94	17.24 ± 3.85	19.80 ± 3.14	47.09 ± 8.64	84.13 ± 15.63
Alkaline earth soil	Alklic Halosols	0.03	0.18 ± 0.08	0.20 ± 0.06	0.33 ± 0.08	0.71 ± 0.22
Alluvial soil	Alluvic Entisols	2.57	8.13 ± 0.68	11.90 ± 1.22	14.82 ± 2.16	34.85 ± 4.06
Bog soil	Orthic Gleysols	0.1	0.58 ± 0.11	0.50 ± 0.07	0.82 ± 0.14	1.90 ± 0.32
Brown calcic soil	Hap-Orthic Aridisols	1.24	1.96 ± 0.74	4.91 ± 2.54	8.71 ± 2.80	15.58 ± 6.08
Brown soil	Hap-Udic Luvisols	0.7	0.02 ± 0.01	0.01 ± 0.01	0.01 ± 0.01	0.04 ± 0.03
Chernozem	Pac-Ustic Isohumosols	0.73	2.77 ± 0.66	2.44 ± 0.50	4.59 ± 0.82	9.80 ± 1.98
Chestnut soil	Cal-Ustic Isohumosols	0.24	1.18 ± 0.00	1.22 ± 0.00	0.42 ± 0.00	2.82 ± 0.00
Chestnut–cinnamon soil	Hap-Ustic Isohumosols	2.63	8.86 ± 0.52	18.65 ± 0.73	33.36 ± 1.57	60.87 ± 2.82
Chisley soil	Lit-Orthic Entisols	1.08	5.18 ± 3.13	0.00 ± 0.00	0.00 ± 0.00	5.18 ± 3.13
Cinnamon soil	Ustic Luvisols	3.17	7.92 ± 0.83	13.29 ± 1.25	26.19 ± 1.61	47.40 ± 3.69
Cold desert soil	Cryic Aridisols	0.2	0.04 ± 0.00	0.05 ± 0.00	0.00 ± 0.00	0.09 ± 0.00
Dark loessial soil	Mat-Cryic Cambisols	2.15	7.06 ± 0.75	9.19 ± 0.85	17.37 ± 1.70	33.62 ± 3.30
Dark felty soil	Typ-Cum-Ustic Isohumosols	0.45	0.00 ± 0.00	0.49 ± 0.49	0.81 ± 0.81	1.30 ± 1.30
Gray desert soil	Hap-Orthic Aridisols	3.45	5.15 ± 1.47	8.79 ± 2.10	17.17 ± 4.31	31.11 ± 7.88
Irrigation-silted soil	Sil-Orthic Anthrosols	1.43	5.44 ± 0.23	9.06 ± 0.27	14.78 ± 0.78	29.28 ± 1.28
Loessial soil	Loe-Orthic Entisols	19.67	94.39 ± 5.88	127.51 ± 4.00	219.18 ± 6.52	441.08 ± 16.40
Lou soil	Earth-cumulic Orthic Anthrosols	1.98	6.59 ± 0.96	7.70 ± 0.90	10.86 ± 2.24	25.15 ± 4.10
Meadow soil	Udic Isohumosols	0.36	1.38 ± 0.33	1.48 ± 0.25	2.17 ± 0.41	5.03 ± 0.99
Moisture soil	Ustic Cambisols	1.87	5.56 ± 0.36	8.97 ± 0.46	15.19 ± 0.85	29.72 ± 1.67
Mountain meadow soil	Cry-Ustic Isohumosols	0.45	0.16 ± 0.15	0.24 ± 0.24	0.41 ± 0.39	0.81 ± 0.78
Paddy soil	Hap-Stagnic Anthrosols	0.08	0.32 ± 0.06	0.63 ± 0.09	0.95 ± 0.20	1.90 ± 0.35
Purple soil	Pur-Orthic Entisols	0.12	0.34 ± 0.00	0.68 ± 0.00	1.17 ± 0.00	2.19 ± 0.00
Red clay	Fer-Udic Luvisols	1.37	4.33 ± 0.92	5.31 ± 1.01	7.91 ± 1.85	17.55 ± 3.78
Saline soil	Orthic Halosols	1.04	3.34 ± 0.93	4.36 ± 0.47	7.39 ± 0.64	15.09 ± 2.04
Sierozem	Cal-Orthic Aridisols	3.26	11.50 ± 0.76	23.00 ± 0.60	36.99 ± 1.57	71.49 ± 2.93
Skeleton soil	Ari-Orthic Entisols	4.2	39.61 ± 16.87	11.44 ± 3.23	0.00 ± 0.00	51.05 ± 20.10
Subalpine meadow soil	Mol-Cryic Cambisols	0.5	0.01 ± 0.01	0.01 ± 0.01	0.00 ± 0.00	0.02 ± 0.02
Total across CLP		62	239 ± 40	292 ± 25	489 ± 40	1020 ± 105

Fig. 5. Spatial distribution of SICD on the CLP at different soil depths of 0–20 cm, 20–50 cm, 50–100 cm and the total layer of 0–100 cm. To generate these maps, the SICD data of the three horizons of the 495 profiles are used in combination with Kriging interpolation to establish the areal ranges over which the profile SICD values cloud be applied.

In the 0–20 cm soil horizon, the SICS of loessial soil (94.39×10^{10} kg) was the highest because this soil occupies the largest area on the CLP. The SICS of skeleton soil (39.61×10^{10} kg) was lower than that of loessial soil. Low SICSs in the 0–20 cm horizon were observed for purple soil, cold desert soil, brown soil, black carpet soil and subalpine meadow soil.

In the 20–50 cm soil horizon, the SICS was very high in loessial soil (127.5×10^{10} kg), and sierozem and eolian sandy soil were higher (23.0×10^{10} kg and 19.8×10^{10} kg, respectively), compared to the

SICS values for the other soil types. Low stocks were observed for cold desert soil, dark felty soil, brown soil, subalpine meadow soil and chisley soil. In the 50–100 cm soil horizon, the two highest SICSs were obtained for loessial soil (219.18×10^{10} kg) and eolian sandy soil (47.09×10^{10} kg). The lower SICSs were found in cold desert soil, skeleton soil and subalpine meadow soil.

The sum of the SICS for all of the soil types in the same horizon can be regarded as the SICS of the corresponding horizon on the CLP. The SICSs in the 0–20, 0–50 and 0–100 cm horizons were estimated to be 2.39, 5.31 and 10.20 Pg, respectively. The SICS in the 0–20, 20–50 and 0–50 cm horizons contributed 23.5, 28.6 and 47.9% respectively of the total CLP SICS. Clearly, the SICS of the different horizons increases with increasing soil depth. This trend is related to the increase in layer thickness and the effect of rainfall. Over time, rainfall caused dissolution and leaching of carbonate in the top horizon and precipitation in the deeper horizons (Mi et al., 2008).

4. Discussion

The SIC density distribution over the CLP is depicted in Fig. 5 for the three standard layers and the total 0–100 cm layer. The maps are based on the SICD values per profile and Kriging interpolation to cover the area between the profile sites. The SICD in the three soil horizons increased with increasing latitude (going north) and decreasing longitude (going west) (Fig. 5), thus showing regional characteristics. In low latitude (southern) regions, the relatively high temperature and abundant rainfall are beneficial for carbonate leaching. Rainfall decreases with

Table 3
Soil carbon stock in the global, in China and in three specific regions of China.

Location	Soil organic carbon stock (Pg C)	Soil inorganic carbon stock (Pg C)	Reference
Global		780–930	Schlesinger (1982)
	1220	720	Sombroek et al. (1993)
	1462–1548	695–748	Batjes (1996)
	1530	940	Eswaran et al. (2000)
China		60	Pan (1999)
	83.8	77.9	Li et al. (2007)
		53.3 ± 6.3	Mi et al. (2008)
		55.3 ± 10.7	Wu et al. (2009)
Desertified land in China	7.84	14.91	Feng et al. (2001)
Tibetan alpine grassland in China	7.36	15.2	Yang et al. (2008) Yang et al. (2010)
Chinese Loess Plateau	4.78	10.20 ± 1.05	Liu et al. (2011) This study

increasing latitude (going north), therefore soil leaching and deposition become weaker at high latitudes (in northern regions), and the SICD increases in these regions. This trend is followed by the SIC stock: the SICS on the CLP increases gradually from east to west and from south to north. The role of rainfall is crucial; comparison of the present results with those Mi et al. (2008) shows that 84.0% of the SIC stock on CLP is concentrated in the area where the annual precipitation is less than 500 mm (Mi et al., 2008).

Finally, it is interesting to consider to what extent the SICS and SOCS contribute to the total soil carbon stock and to compare the CLP with other regions and the overall values for China and globally. To this order the known literature values on SICS and SOCS are collected in Table 3. The global SOCS estimates range from 1220 to 1548 Pg C, while the global SICS estimates range from 695 to 940 Pg C; i.e., approximately 60% of the global soil carbon stock consists of SOC and approximately 40% consists of SIC. For China, the SOCS estimates are approximately 83.8 Pg C and the SICS estimates range from 53.3 to 77.9 Pg C. Therefore, also in China the SOC stock is substantially higher than the SIC stock. The total carbon stocks in all of China can also be compared with those in the arid and semi-arid regions of China. Due to the large area of the CLP and the relatively high SICD of the soils, the SIC stock of the CLP is high. The presently calculated SICS of the CLP is 10.20 Pg C, this is 2.1 times more than SOCS on the CLP (Liu et al., 2011). The SICS and SOCS of the 0–100 cm horizon in the desert region of northern China are 14.91 and 7.84 Pg C, respectively (Feng et al., 2001), i.e., here SICS is 1.8 times the SOCS. The SICS of the grassland on the Tibetan Plateau was found to be 15.2 Pg C, which is 2.1 times higher than the corresponding SOCS (Yang et al., 2010). Evidently, due to the dry conditions, the SICS/SOCS ratio in the arid and semi-arid regions is much higher than the Chinese and global SICS/SOCS ratio.

The SICS of 10.20 Pg C on the CLP accounts for about 18.4% of the SICS in China (60 Pg C), whereas the area of the CLP only accounts for 6.6% of the national area. Additionally, the desert areas and the Tibetan alpine grassland contribute considerably to the national SICS (Table 3). This indicates that the SICS on the CLP and in the arid and semi-arid regions in China are relatively important to the terrestrial carbon cycle of China.

Soil inorganic carbon plays a very important role in the global carbon cycle and climate change; therefore, estimates of SICSs are vitally important (Wu et al., 2001). The large scale (global or China) estimates of SICD and SICS reported in literature, however, differ substantially (Table 3). Estimations of soil carbon stocks are usually focused on a soil profile depth of 100 cm, however, in some regions with exceptionally large SOCS and SICS, the whole soil profile depth is much larger. Therefore, to assess the potential influence of soil on the terrestrial carbon cycle, the common practice to mainly study the 0–100 cm layer should be avoid in future studies and the whole soil layer should be taken into account. This also applies to the CLP where at most locations the soil layer also exceeds the 100 cm depth considerably.

4. Conclusions

Based on the data from the Chinese Second National Soil Survey, the SIC density and SIC stock in the top 100 cm for the different soil types and land use patterns across the CLP were estimated to 17.04 kg/m^2 and 10.20 Pg C, respectively. Detailed analysis of the horizons 0–20 cm, 20–50 cm and 50–100 cm showed that the SICD increased with depth for all soil types and land use patterns, and the magnitude and vertical distribution of the SICD were related to the climate conditions. The SICD and SICS values in the CLP soils were approximately 2.2 and 2.1 times higher than the SOCD and SOCS values, respectively. The SICS represented approximately 18.4% of the overall SICS in China, indicating that the SIC stock of the CLP makes a significant contribution to China's terrestrial carbon balance.

References

Adams, J.M., 1993. Caliche and the carbon cycle. Nature 361, 213–214.
Batjes, N.H., 1996. Total carbon and nitrogen in the soils of world. Eur. J. Soil Sci. 47, 151–163.
Black, G.R., Hartge, K.H., 1986. Bulk density, In: Klute, A. (Ed.), Methods of Soil Analysis. Part 1, Physical and Mineralogical Methods, 2nd ed. ASA and SSSA, Madison, WI, pp. 363–375.
Bowman, W.D., Cleveland, C.C., Halada, L., Hreško, J., Baron, J.S., 2008. Negative impact of nitrogen deposition on soil buffering capacity. Nat. Geosci. 1, 767–770.
Cooperative Research Group on Chinese Soil Taxonomy (CRGCST), 2001. Chinese Soil Taxonomy, 3rd edition. Science Press, Beijing.
Cressie, N., 1993. Statistics for Spatial Data. Wiley-InterScience, New York.
Dreimanis, A., 1962. Quantitative gasometric determination of calcite and dolomite by using Chittick apparatus. J. Sediment. Res. 32, 520–529.
Emmerich, W.E., 2003. Carbon dioxide fluxes in a semiarid environment with high carbonate soils. Agric. For. Meteorol. 116, 91–102.
Entry, J.A., Sojka, R.E., Shewmaker, G.E., 2004. Irrigation increases inorganic carbon in agricultural soils. Environ. Manag. 33, 309–317.
Eswaran, H., Van Den Berg, E., Reich, P., 1993. Organic carbon in soils of the world. Soil Sci. Soc. Am. J. 192–194.
Eswaran, H., Reich, P.F., Kimble, J.M., Beinroth, F.H., Padmanabhan, E., Moncharoen, P., 2000. Global carbon stocks. In: Lal, R., Kimble, J.M., Eswaran, H., Stewart, B.A. (Eds.), Global Change and Pedogenic Carbonate. CRC Press, Boca Raton, FL, pp. 15–25.
Fang, J.Y., Chen, A.P., Peng, C.H., Zhao, S.Q., Ci, L.J., 2001. Changes in forest biomass carbon storage in China between 1949 and 1998. Science 292, 2320–2322.
Feng, Q., Cheng, G.D., Endo, K., 2001. Carbon storage in the desertified lands: a case study from North China. GeoJournal 51, 181–189.
Goddard, M.A., Mikhailova, E.A., Post, C.J., Schlautman, M.A., 2007. Atmospheric Mg^{2+} wet deposition within the continental United States and implications for soil inorganic carbon sequestration. Tellus 59B, 50–56.
He Nan Soil Survey Office (HNSSO), 2004. Soils of Henan Province in China. China Agricultural Press, Beijing (in Chinese with English abstract).
Inner Mongolia Autonomous Region's Soil Survey Office (IMARSSO), 1994. Soil Species of Inner Mongolia Autonomous Region's in China. China Agricultural Press, Beijing (in Chinese with English abstract).
Jobbágy, E.G., Jackson, R.B., 2000. The vertical distribution of soil organic carbon and its relation to climate and vegetation. Ecol. Appl. 10, 423–436.
Lal, R., 2004. Soil carbon sequestration to mitigate climate change. Geoderma 123, 1–22.
Lal, R., Kimble, J.M., 2000. Pedogenic carbonates and the global carbon cycle. In: Lal, R., Kimble, J.M., Eswaran, H., Stewart, B.A. (Eds.), Global Climate Change and Pedogenic Carbonates. CRC Press, Boca Raton, FL, pp. 1–14.
Li, Z.P., Han, F.X., Su, Y., Zhang, T.L., Sun, B., Monts, D.L., Plodinec, M.J., 2007. Assessment of soil organic and carbonate carbon storage in China. Geoderma 138, 119–126.
Li, M., Zhang, X., Pang, G., Han, F., 2013. The estimation of soil organic carbon distribution and storage in a small catchment area of the Loess Plateau. Catena 101, 11–16.
Liu, Y.Z., Zhang, J.Y., 1992. Soils of Shaanxi Province. Science Press, Beijing (in Chinese with English abstract).
Liu, D.W., Wang, Z.M., Zhang, B., Song, K.S., Li, X.Y., Li, J.P., Li, F., Duan, H.T., 2006. Spatial distribution of soil organic carbon and analysis of related factors in croplands of the black soil region, Northeast China. Agric. Ecosyst. Environ. 113, 73–81.
Liu, Z.P., Shao, M.A., Wang, Y.Q., 2011. Effect of environmental factors on regional soil organic carbon stocks across the Loess Plateau region, China. Agric. Ecosyst. Environ. 142, 184–194.
Mi, N., Wang, S.Q., Liu, J.Y., Yu, G.R., Zhang, W.J., Jobbágy, E., 2008. Soil inorganic carbon storage pattern in China. Glob. Chang. Biol. 14, 2380–2387.
Mielnick, P., Dugas, W.A., Mitchell, K., Havstad, K., 2005. Long-term measurements of CO$_2$ flux and evapotranspiration in a Chihuahuan desert grassland. J. Arid Environ. 60, 423–436.
Mikhailova, E.A., Post, C.J., 2006. Effects of land use on soil inorganic carbon stocks in the Russian Chernozem. J. Environ. Qual. 35, 1384–1388.
Ming, D.W., 2002. Carbonates. In: Lal, R. (Ed.), Encyclopedia of Soil Science. Marcel Dekker Inc., New York, pp. 139–141.
National Soil Survey Office (NSSO), 1995a. Soil Species of China, vol. 4. China Agricultural Press, Beijing (in Chinese with English abstract).
National Soil Survey Office (NSSO), 1995b. Soil Species of China, vol. 5. China Agricultural Press, Beijing (in Chinese with English abstract).
National Soil Survey Office (NSSO), 1998. Soils of China. China Agricultural Press, Beijing (in Chinese with English abstract).
Palmer, C.J., Smith, W.D., Conkling, B.L., 2002. Development of a protocol for monitoring status and trends in forest soil carbon at a national level. Environ. Pollut. 116 (Suppl. 1), 209–219.
Pan, G.X., 1999. Study on carbon reservoir in soils of China. Bull. Sci. Technol. 15, 330–332 (in Chinese with English abstract).
Pan, G.X., Cao, J.H., Zhou, Y.C., 2000. Soil carbon and its significance in carbon cycling of earth surface system. Quat. Sci. 20, 325–334 (in Chinese with English abstract).

Papiernik, S.K., Lindstrom, M.J., Schumacher, J.A., Malo, D.D., Lobb, D.A., 2007. Characterization of soil profiles in a landscape affected by long-term tillage. Soil Tillage Res. 93, 335–345.

Qinghai Agricultural Resources and Regional Planning Office (QARRPO), 1995. Soil Species of Qinghai. China Agricultural Press, Beijing (in Chinese with English abstract).

Sartori, F., Lal, R., Ebinger, M.H., Eaton, J.A., 2007. Changes in soil carbon and nutrient pools along a chronosequence of poplar plantations in the Columbia Plateau, Oregon, USA. Agric. Ecosyst. Environ. 122, 325–339.

Scharpenseel, H.W., Mtimet, A., Freytag, J., 2000. Soil inorganic carbon and global change. In: Lal, R., Kimble, J.M., Eswaran, H., Stewart, B.A. (Eds.), Global Climate Change and Pedogenic Carbonates. CRC Press, Boca Raton, FL, pp. 27–42.

Schlesinger, W.H., 1982. Carbon storage in the caliche of arid soils: a case of study from Arizona. Soil Sci. 133, 247–255.

Schlesinger, W.H., 2002. Inorganic carbon and the global carbon cycle. In: Lal, R. (Ed.), Encyclopedia of Soil Science. Marcel Dekker Inc., New York, pp. 706–708.

Shi, H., Shao, M.A., 2000. Soil and water loss from the Loess Plateau in China. J. Arid Environ. 45, 9–20.

Singh, S.K., Sharma, B.K., Singh, A.K., Tarafdar, J.C., 2007. Carbon stock and organic carbon dynamics in soils of Rajasthan, India. J. Arid Environ. 68, 408–421.

Sombroek, W.G., Nachtergaele, F.O., Hebel, A., 1993. Amounts, dynamics and sequestrations of carbon in tropical and subtropical soils. Ambio 22, 417–426.

Velde, B., Meunier, A. (Eds.), 2008. The Origin of Clay Minerals in Soils and Weathered Rocks. Springer-Verlag, Berlin Heidelberg.

Walkley, A., Black, I.A., 1934. An examination of the Degtjareff method for determining soil organic matter and a proposed modification of the chromic acid titration method. Soil Sci. 37, 29–38.

Wang, S.Q., Zhou, C.H., 1999. Estimating soil carbon reservoir of terrestrial ecosystem in China. Geogr. Res. 18, 349–356.

Wang, Y.Q., Shao, M.A., Liu, Z.P., 2010. Large-scale spatial variability of dried soil layers and related factors across the entire Loess Plateau of China. Geoderma 159, 99–108.

Wang, Y., Fu, B., Lue, Y., Chen, L., 2011. Effects of vegetation restoration on soil organic carbon sequestration at multiple scales in semi-arid Loess Plateau, China. Catena 85, 58–66.

Wang, Z., Liu, G.B., Xu, M.X., Zhang, J., Wang, Y., Tang, L., 2012. Temporal and spatial variations in soil organic carbon sequestration following revegetation in the hilly Loess Plateau, China. Catena 99, 26–33.

Wang, Z.P., Han, X.G., Chang, S.X., Wang, B., Yu, Q., Hou, L.Y., Li, L.H., 2013. Soil organic and inorganic carbon contents under various land uses across a transect of continental steppes in Inner Mongolia. Catena 109, 110–117.

Wen, Q.Z., 1989. Geochemistry of the Chinese Loess. Science Press, Beijing (in Chinese with English abstract).

Weng, J.T., 1995. The effect of carbon rocks on global carbon cycle. Adv. Earth Sci. 10, 154–158 (in Chinese with English abstract).

Wu, H.B., Guo, Z.T., Peng, C.H., 2001. Changes in terrestrial carbon storage with global climate changes since the last interglacial. J. Quat. Sci. 21, 366–376 (in Chinese with English abstract).

Wu, H.B., Guo, Z.T., Peng, C.H., 2003. Land use induced changes of organic carbon storage in soils of China. Glob. Chang. Biol. 9, 305–315.

Wu, H.B., Guo, Z.T., Gao, Q., Peng, C.H., 2009. Distribution of soil inorganic carbon storage and its changes due to agricultural land use activity in China. Agric. Ecosyst. Environ. 129, 413–421.

Xu, S.Y., He, S.Y., 1996. The CO_2 regime of soil profile and its drive to dissolution of carbonate rock. Carsologica Sinica 15, 50–57.

Xu, N.Z., Zhang, T.L., Wang, X.X., Liu, H.Y., Liang, X.H., 2009. Statistical calculation of soil inorganic carbon stock in the Yangtze delta region. Resour. Environ. Yangtze Basin 18, 1038–1044 (in Chinese with English abstract).

Yang, W.Z., Shao, M.A., 2000. Soil Water Research on the Loess Plateau. Science Press, Beijing (in Chinese with English abstract).

Yang, Y.H., Fang, J.Y., Tang, Y.H., Ji, C.J., Zheng, C.Y., He, J.S., Zhu, B., 2008. Storage, patterns and controls of soil organic carbon in the Tibetan grasslands. Glob. Chang. Biol. 14, 1592–1599.

Yang, Y.H., Fang, J.Y., Ji, C.J., Ma, W.H., Su, S.S., Tang, Z.Y., 2010. Soil inorganic carbon stock in the Tibetan alpine grasslands. Global Biogeochem. Cycles 24, GB4022. http://dx.doi.org/10.1029/2010GB003804.

Yang, Y.H., Fang, J.Y., Ji, C.J., Ma, W.H., Mohammat, A., Wang, S.F., Wang, S.P., Datta, A., Robinson, D., Smith, P., 2012. Widespread decreases in topsoil inorganic carbon stocks across China's grasslands during 1980s–2000s. Glob. Chang. Biol. 18, 3672–3680.

Yu, D.S., Shi, X.Z., Wang, H.J., Sun, W.X., Chen, J.M., Liu, Q.H., Zhao, Y.C., 2007a. Regional patterns of soil organic carbon stocks in China. J. Environ. Manag. 85, 680–689.

Yu, D.S., Shi, X.Z., Wang, H.J., Sun, W.X., Warner, E.D., Liu, Q.H., 2007b. National scale analysis of soil organic carbon storage in China based on Chinese soil taxonomy. Pedosphere 17, 11–18.